Inorganic Chemistry

Article

pubs.acs.org/IC

Syntheses, Structures, and Magnetic and Luminescence Properties of a New Dy^{III}-Based Single-Ion Magnet

Ya-Li Wang,[†] Yue Ma,*[,†] Xi Yang,[†] Jinkui Tang,*[,‡] Peng Cheng,[†] Qing-Lun Wang,[†] Li-Cun Li,[†] and Dai-Zheng Liao[†,§]

[†]Department of Chemistry and Key Laboratory of Advanced Energy Materials Chemistry (MOE) and TKL of Metal and Molecule Based Material Chemistry, Nankai University, Tianjin 300071, P.R. China

[‡]State Key Laboratory of Rare Earth Resource Utilization, Changchun Institute of Applied Chemistry, Chinese Academy of Sciences, Changchun 130022, P.R. China

[§]State Key Laboratory of Physical Chemistry of Solid Surface, Xiamen University, Xiamen 361005, P.R. China

Supporting Information

ABSTRACT: Three new Ln^{III} complexes based on 2,2′-bipyridine $[Ln(hfac)_3(bpy)]$ (Ln = Dy (**1**), Tb (**2**), or Ho (**3**); hfac = hexafluoroacetylacetonate; and bpy = 2,2′-bipyridine) have been synthesized and characterized structurally and magnetically. Single-crystal X-ray analysis shows that all these complexes contain one $[Ln(hfac)_3(bpy)]$ unit in which a center Ln^{III} ion is surrounded with a slightly distorted square-antiprismatic LnO_6N_2 coordination sphere formed by three bischelate hfac anions and one bpy ligand. Both static and dynamic magnetic properties were studied for complex **1**, which is proved to be a new single-ion magnet. The luminescence characterizations of complexes **1** and **2** are also studied in this paper.

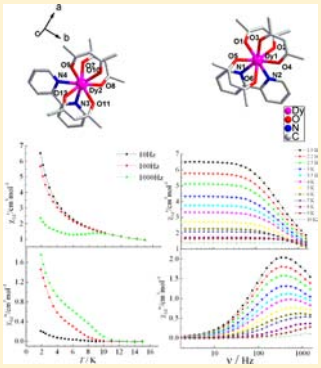

INTRODUCTION

With an improved knowledge of the magneto-chemical properties of single-molecule magnets (SMMs), lanthanide (Ln) ions have become attractive candidates for constructing new SMMs because most of them have a large unquenched orbital angular momentum,[1] which may bring significant anisotropy to the system. In fact, a mononuclear lanthanide compound in which the anisotropic ion lies in an axial crystal field environment can exhibit slow relaxation of the magnetization,[2,3] so the interest in single-ion magnets (SIMs) has rapidly developed because of the simplification of the analysis of local anisotropy.[4] Synthetic efforts along this line have led to the discovery of many SIMs, including lanthanide complexes with phthalocyanine,[2] polyoxometalate,[3,5] or macrocyclic Schiff base ligands,[6] β-diketone[1e,7,8] or organometallic systems,[9] nitronyl nitroxide radicals,[10] or DOTA ligands.[4d]

Notably, the ligand field (LF) is a key player in controlling the magnetic anisotropy of Ln-based SIMs.[1f,8a] Careful manipulation of the ligand system can produce a desirable LF, which would further affect the splitting of the ground J multiplet and give the lowest sublevels a large $|J_z|$ value and significant energy gap from the rest of the sublevels, thus achieving an easy axis of the magnetization. The material $Dy(hfac)_3{\cdot}2H_2O$ has been confirmed to show practically no SMM behavior,[11] so investigating whether a small change of the coordination sphere would affect the magnetic properties attracted us. Considering the above, by adopting 2,2′-bipyridine (bpy) to the system of $Ln(hfac)_3{\cdot}2H_2O$, we report the syntheses, structures, and magnetic properties of three lanthanide mononuclear compounds, $[Ln(hfac)_3(bpy)]$ (Ln = Dy (**1**), Tb (**2**), or Ho (**3**)). Among them, complex **1** shows the typical features associated with the SIM behavior. In addition, lanthanides are widely studied for their specific luminescence properties, especially in the aromatic or heteroaromatic highly π-conjugated system and/or the β-diketone system.[12] Herein, we present the luminescence spectra and the quantum yields of the complexes.

EXPERIMENTAL SECTION

Materials and Measurements. All of the reagents used in the syntheses are of analytical grade, except the *n*-heptane which was dried over sodium and distilled prior to use. The hexafluoroacetylacetone and 2,2′-bipyridine were purchased from Alfa Chemical Company. Elemental analysis for C, H, and N was performed on a Perkin-Elmer elemental analyzer, model 240. Luminescence spectra and luminescence quantum yields were determined on solid samples with a FL3-2-IHR320-NIR-TCSPC spectrofluorimeter at 295 K. Variable-temperature magnetic susceptibilities were measured on a SQUID MPMS XL-7 magnetometer in the range of 2−300 K. Diamagnetic corrections were made with Pascal's constants for all of the constituent atoms.[13]

Syntheses of $[Ln(hfac)_3(bpy)]$ (Ln = Dy (1), Tb (2), or Ho (3)). All three of the complexes were synthesized by the same method. The

Received: January 2, 2013
Published: June 7, 2013

dx.doi.org/10.1021/ic400006n | Inorg. Chem. 2013, 52, 7380−7386

Table 1. Crystal Data and Structure Refinements for Complexes 1−3

	1	2	3
empirical formula	$C_{25}H_{11}F_{18}DyN_2O_6$	$C_{25}H_{11}F_{18}TbN_2O_6$	$C_{25}H_{11}F_{18}HoN_2O_6$
formula weight	939.86	936.29	942.29
temperature (K)	113(2)	113(2)	113(2)
crystal system	monoclinic	triclinic	monoclinic
space group	$P_{21/c}$	$\bar{P}1$	$P_{21/c}$
a (Å)	21.346(4)	11.793(2)	21.297(4)
b (Å)	18.782(4)	15.860(3)	18.783(4)
c (Å)	16.033(3)	17.825(4)	16.013(3)
α (deg)	90	78.93(3)	90
β (deg)	106.14(3)	77.25(3)	106.06(3)
γ (deg)	90	72.95(3)	90
volume (Å^3)	6175(2)	3079.7(12)	6156(2)
Z	8	4	8
ρ_{calc} (g cm^{-3})	2.022	2.019	2.033
μ (mm^{-1})	2.572	2.449	2.723
F(000)	3608	1800	3615
reflections collected	55351	22457	40987
unique/parameters	14656/1133	10737/1077	10838/1105
R(int)	0.0435	0.0293	0.0398
completeness to θ = 27.48	99.5%	99.0%	99.8%
max/min transmission	0.734/0.636	0.710/0.631	0.721/0.586
goodness-of-fit on F^2	1.058	1.061	1.044
R_1, wR_2 [$I > 2\sigma(I)$]	0.0581, 0.1478	0.0485, 0.1336	0.0436, 0.1090
R_1, wR_2 (all data)	0.0688, 0.1663	0.0562, 0.1398	0.0503, 0.1140

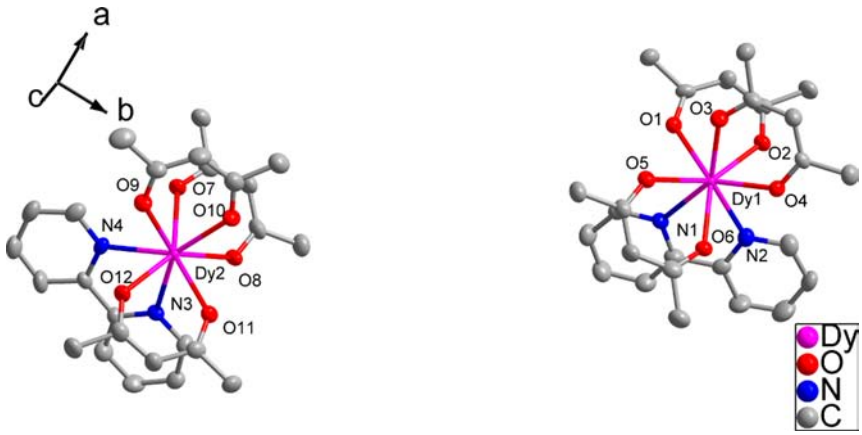

Figure 1. Molecular structure of complex **1** with thermal ellipsoids at 30% probability. Hydrogen and fluorine atoms are omitted for clarity.

synthesis of compound **1** is detailed herein. Dy(hfac)$_3$·2H$_2$O (0.082 g, 0.1 mmol) was dissolved in 20 mL of dry boiling *n*-heptane. A 5 mL CH_2Cl_2 solution of 2,2′-bipyridine (0.0156 g, 0.1 mmol) was added, and the mixture was heated for 30 min at around 60 °C. Pale-yellow crystals of **1** suitable for X-ray analysis were isolated by cooling the solution to room temperature and keeping the filtrate in a refrigerator at 4 °C for a week. Anal. Calcd (**1**) for $C_{25}H_{11}F_{18}DyN_2O_6$ (yield 0.0389 g, 41.4%): C, 31.95; H, 1.18; N, 2.98. Found: C, 31.84; H, 1.38; N, 2.81. IR (KBr cm^{-1}): 1652 (vs), 1642 (s), 1556 (w), 1508 (s), 1458 (w), 1254 (vs), 1212 (s), 1094 (w), 804 (m). Anal. Calcd (**2**) for $C_{25}H_{11}F_{18}TbN_2O_6$ (yield 0.0315 g, 33.6%): C, 32.07; H, 1.18; N, 2.99. Found: C, 32.19; H, 1.02; N, 3.08. IR (KBr cm^{-1}): 1654 (vs), 1642 (s), 1546 (s), 1391 (w), 1256 (vs), 1205 (s), 1097 (w), 805 (m). Anal. Calcd (**3**) for $C_{25}H_{11}F_{18}HoN_2O_6$ (yield 0.0271 g, 28.8%): C, 31.87; H, 1.18; N, 2.97. Found: C, 31.76; H, 1.24; N, 2.89. IR (KBr cm^{-1}): 1655 (vs), 1645 (s), 1548 (s), 1395 (w), 1252 (vs), 1204 (s), 1149 (w), 802 (m).[12d]

X-ray Crystallography. Determination of the unit cell and data collection for the complexes were performed with Mo Kα radiation (λ = 0.71073 Å) on a Rigaku MM-007 single-crystal diffractometer at 113(2) K. All of the structures were solved primarily by direct methods and refined with full-matrix least-squares techniques using the SHELXS-97 and SHELXL-97 programs.[14] All non-hydrogen atoms were refined with anisotropic thermal parameters. The hydrogen atoms were introduced in calculated positions and refined with a fixed geometry with respect to their carrier atoms.[15] Crystal data and details of structural determination refinement are summarized in Table 1, and the selected bond lengths and angles have been provided in the Supporting Information, Tables S1−S3. CCDC 783498, 784030, and 784031 contain the supplementary crystallographic data for complexes **1**−**3**, respectively. These data can be obtained free of charge from the Cambridge Crystallographic Data Center via www.ccdc.cam.ac.uk/data_request/cif.

RESULTS AND DISCUSSION

Description of Crystal Structure. Single-crystal X-ray diffraction analysis revealed that **1** and **3** crystallize in the monoclinic $P_{21/c}$ space group, whereas **2** crystallizes in the triclinic $\bar{P}1$ space group. They have similar structures, all

dx.doi.org/10.1021/ic400006n | Inorg. Chem. 2013, 52, 7380−7386

consisting of two crystallographically independent [Ln(hfac)$_3$(bpy)] moieties in one unit. The center Ln^{III} ions all have a similar distorted square-antiprismatic LnO_6N_2 coordination sphere formed by three hfac anions and a bipyridine ligand, with only little difference in the bond lengths and angles. Therefore, only the structure of Dy^{III} complex **1** is described in detail (as shown in Figure 1). In the [Dy(hfac)$_3$(bpy)] unit, each hfac anion provides two donor oxygen atoms coordinating to the Dy^{III} cation, and the other two coordination sites of Dy^{III} are occupied by the two N atoms from bipyridine to complete the eight-coordination environment DyO_6N_2. The Dy−O distances range from 2.314 to 2.359 Å for Dy1 and 2.321 to 2.358 Å for Dy2, while the two Dy−N bonds are 2.505 and 2.513 Å for Dy1 and 2.505 and 2.517 Å for Dy2. Eight-coordinated geometries are mostly taken as the D_{2d}-dodecahedron (DD), C_{2v}-bicapped trigonal prism (TP), and D_{4d}-square antiprism (SAP). The semiquantitative method of polytopal analysis is examined.[10e,16] The polyhedrons with donor atoms around the lanthanide center for the complex are shown in the Supporting Information, Scheme S1. Relevant dihedral angles are summarized in Table 2. The δ_1 and δ_2 values, which represent planarity of the squares, range from 1.32 to 7.93°. The δ_3 and δ_4 values for the triangular faces, along with φ values, are close to the angles (52.4, 52.4, and 24.5°) of an ideal SAP polyhedron, respectively, indicative of D_{4d} symmetry (Supporting Information, Figure S1). In addition, the interplanar distances between the coordination planes above and below the lanthanide ion in the SAP polyhedron are 3.335 Å for Dy1 and 2.780 Å for Dy2, which are indicative of a certain axial elongation of the square antiprism for Dy1 and axial compression for Dy2.[3a] The shortest Dy−Dy distance is 7.92 Å for complex **1**, and the packing diagram for **1** is given in the Supporting Information, Figures S2 and S3. Meanwhile, weak C−H···F hydrogen bonds were found in the complex with H···F distances ranging from 2.35 to 2.48 Å.[12f]

Table 2. δ (deg) and φ (deg) Values for Complex 1[a]

	1-Dy1		1-Dy2		SAP	TP	DD
δ_1	O5−[O3−O6]−O4	1.3	O9−[O10−O12]−O11	2.8	0.0	0.0	29.5
δ_2	O1−[N1−O2]−N2	5.3	O7−[N4−O8]−N3	7.9	0.0	21.8	29.5
δ_3	O5−[N1−O6]−N2	44.8	O9−[N4−O12]−N3	56.6	52.4	48.2	29.5
δ_4	O1−[O3−O2]−O4	46.1	O7−[O10−O8]−O11	58.5	52.4	48.2	29.5
φ_1	O6−O2−O5−O1	19.8	O12−[O8−O9]−O7	30.2	24.5	14.1	0.0
φ_2	O3−N1−O4−N2	17.2	O10−[N4−O11]−N3	30.0	24.5	14.1	0.0

[a]A[BC]D is the dihedral angle between the ABC plane and the BCD plane. A−B−C−D is the dihedral angle between the (AB)CD plane and the AB(CD) plane, where (AB) is the center of A and B.

Luminescence Properties. The photoluminescence of complexes **1** and **2** in the solid state was investigated under excitation at 355 nm at room temperature. The typical luminescence peaks of Dy^{III} at 481 and 574 nm can be assigned to the transitions of $^4F_{9/2} \rightarrow {}^6H_{15/2}$ and $^4F_{9/2} \rightarrow {}^6H_{13/2}$, respectively (Figure 2a). The yellow emission intensity of the $^4F_{9/2} \rightarrow {}^6H_{13/2}$ transition is much stronger than that of the blue $^4F_{9/2} \rightarrow {}^6H_{15/2}$ transition, suggesting that the ligand is suitable for the sensitization of yellow luminescence of Dy^{III}, as are those in other similar complexes.[4c] For Tb^{III} ions, the first emission band of complex **2** at 489 nm can be assigned to the transitions of $^5D_4 \rightarrow {}^7F_6$, while the other bands at 545, 580, and 617 nm can be attributed to the $^5D_4 \rightarrow {}^7F_5$, $^5D_4 \rightarrow {}^7F_4$, and $^5D_4 \rightarrow {}^7F_3$ transitions, respectively (Figure 2b).[12c,e] Among them, the $^5D_4 \rightarrow {}^7F_5$ transition is the strongest. For the ligand (bpy), the broad emission band observed from 255 to 450 nm can be attributed to the $\pi \rightarrow \pi^*$ transition of the ligand (Supporting Information, Figure S4).[12c]

The luminescence quantum yields of complexes **1** and **2** were also determined by means of an integrating sphere at room temperature under the excitation wavelength that maximizes the emissions of the lanthanide ions. The solid-state measurement gave a quantum yield of 0.4% for Dy^{III} complex **1** and 3.4% for Tb^{III} complex **2**, which is near the 0.75% measurement previously reported for [Tb(hfa)$_3$(bpyO2)] (hfa = hexafluoroacetylacetonate; bpyO2 = 2,2′-bipyridine-*N*,*N*′-dioxide) but much lower than the value of 27% reported for [Tb(hfa)$_3$(H$_2$O)$_2$].[12g] It shows that, similar to bpyO2, the ancillary ligand of bpy also has a detrimental effect on the luminescence of the Tb^{III} complex, which arises from the close energetic proximity of the ligand triplet state and the $^5D_4$ level.

Magnetic Properties. *Static Magnetic Properties for 1.* Direct current (dc) magnetic susceptibility studies of **1** were carried out in an applied magnetic field of 1000 Oe over the temperature range 2−300 K. At room temperature, the $\chi_M T$

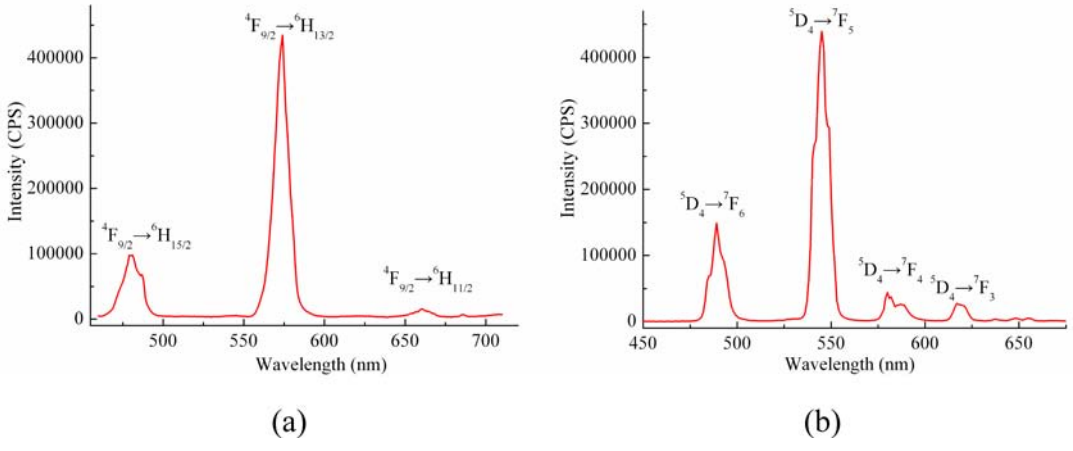

Figure 2. Upon excitation at 355 nm, room-temperature solid-state luminescence spectra of **1** (a) and **2** (b).

dx.doi.org/10.1021/ic400006n | Inorg. Chem. 2013, 52, 7380−7386

value of 14.26 cm^3 K mol^{-1} is in good agreement with the theoretical value of 14.16 cm^3 K mol^{-1} for one uncoupled Dy^{III} ion (S = 5/2, L = 5, $^6H_{15/2}$, g = 4/3). As shown in Figure 3,

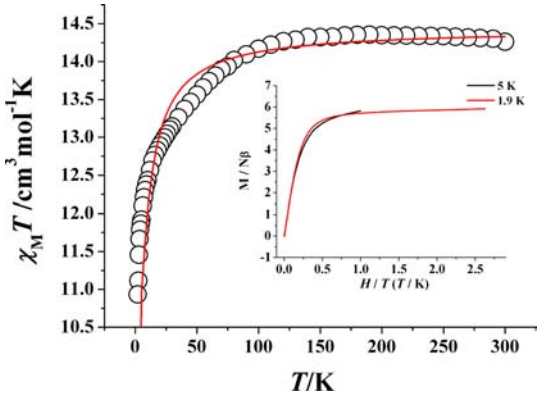

Figure 3. Temperature dependence of $\chi_M T$ product in the range of 2–300 K in 1000 Oe for **1**. The solid line represents the theoretical data. Inset: M vs H/T plot measured at different temperatures.

during the cooling process, the $\chi_M T$ has almost no change in the temperature range of 300–100 K and then decreases gradually, which is mostly due to crystal field effects (i.e., thermal depopulation of the Ln^{III} Stark sublevels), and then further decreases sharply to reach a minimum of 10.93 cm^3 K mol^{-1} at 2 K, which is mostly due to an almost pure $|m_j = \pm 15/2\rangle$ ground-state doublet[17] and possible dipole–dipole interactions between the molecules. The magnetic susceptibility was simulated by an approximate model, described in detail in the Supporting Information, because there is very weak magnetic interaction between Dy^{III} ions in complex **1**.

The M versus H/T data measured in different magnetic fields (inset Figure 3) show nonsuperposition, suggesting the presence of magnetic anisotropy and/or low-lying excited states. The maximum magnetization at 2 and 5 K is 5.93 μ_B, which is lower than the expected saturation value of 10 μ_B for each Dy^{III} ion, most likely because of the crystal field effect at the Dy^{III} ion that eliminates the 16-fold degeneracy of the $^6H_{15/2}$ ground state.[18]

Dynamic Magnetic Properties for 1. The temperature and frequency dependency data of the alternating current (ac) susceptibilities for **1** under zero-dc field (Figure 4) show strong frequency and temperature dependencies. From the temperature dependencies of the ac susceptibility (Figure 4, left), both the in-phase (χ') and out-of-phase (χ'') signals show a maximum, while the peaks can be found only at frequencies higher than 1000 Hz. As cooling continues, χ' and χ'' start to increase again below 4 K. This behavior is typical of the quantum tunneling regime often seen in Dy^{III}-based SMMs.[2b,8b,10b,18b]

From frequency dependencies of the ac susceptibility (Figure 4, right), the magnetization relaxation times (τ) have been estimated between 2 and 10 K (Figure 5). Above 8 K, the

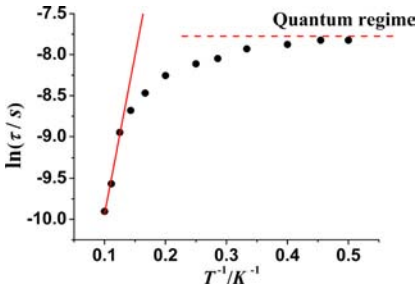

Figure 5. Magnetization relaxation time, ln τ vs T^{-1} plot for **1** under zero-dc field. The solid line is fitted with the Arrhenius law (see text). With $\tau_0 = 1.12 \times 10^{-6}$ s, U = 38.48 K.

relaxation follows a thermally activated mechanism affording an energy barrier of 38.48 K with a pre-exponential factor (τ_0) of 1.12×10^{-6} s based on Arrhenius law [$\tau = \tau_0 \exp(U_{eff}/k_B T)$], which is consistent with those reported for similar SMMs (in the $\sim 10^{-6}$–10^{-11} s range).[7,8,10] While at lower temperatures a gradual crossover to a temperature-independent regime is observed. Below about 2.2 K, a dominant temperature-independent quantum regime of dynamics with a τ value of

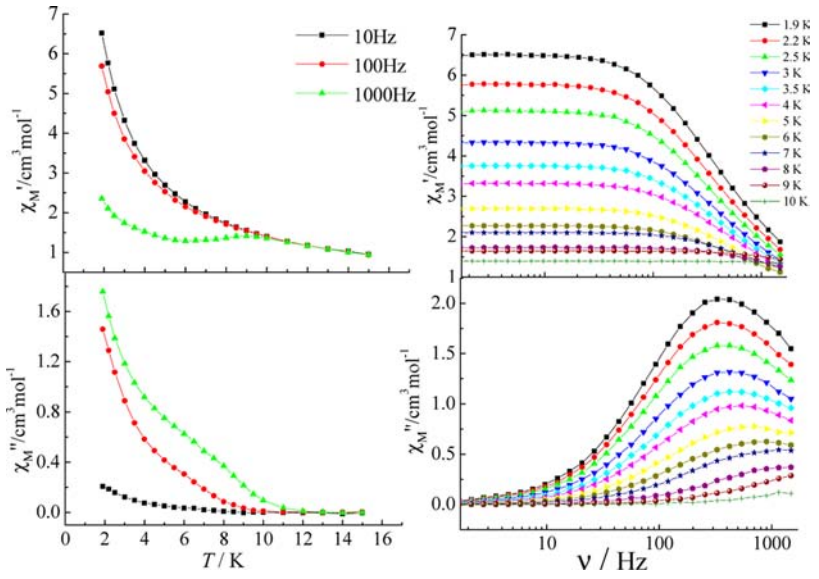

Figure 4. Temperature (left) and frequency (right) dependence of the ac susceptibility for complex **1** as a function of the temperature below 15 K (left) and the ac frequency between 1 and 1500 Hz (right) under a zero-dc field.

dx.doi.org/10.1021/ic400006n | Inorg. Chem. 2013, 52, 7380–7386

0.0004 s explains the absence of the M versus H hysteresis effect at 1.9 K (Supporting Information, Figure S5). This may be due to the hyperfine couplings and dipolar spin−spin interactions in lanthanide ions, which allow fast quantum tunneling of magnetization (QTM)[5b,8a,19] that prevents the isolation of zero-field lanthanide SMMs with large barriers.[20]

From frequency dependencies of the ac susceptibility measurements, Cole−Cole diagrams (Figure 6) in the form of χ'' versus χ' with nearly semicircular shapes have also been obtained. These data have been fitted to the generalized Debye model,[21] giving the small distribution coefficient α value 0.137−0.150 (between 1.9 and 6.0 K), indicating the narrow distribution of relaxation times at these temperatures.

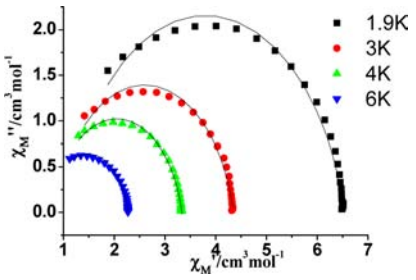

Figure 6. Cole−Cole plots measured at 1.9−6 K in zero-dc field. The solid lines are the best fit to the experimental data, obtained with the generalized Debye model with α = 0.137−0.150.

To further ensure that complex **1** is a SMM, the indicative parameter of spin disorder ϕ of 0.21 can be extracted on the basis of the temperature dependency data of χ' using Mydosh's formula $\phi = (\Delta T_p/T_p)/\Delta(\log \omega)$, which finally excluded the possibility of a spin glass ($0.01 < \phi < 0.08$).[22,23]

All the above magnetic analysis evidences the SIM behavior for the Dy^{III} complex, which basically originates from intrinsic molecular properties of the complex. Single-ion anisotropy of the 4f ions is probably the most important factor, owing to the strength and symmetry of the local crystal field. It could be considered that high symmetry environments around the Dy^{III} ion favor high blocking temperature.[2a,3a,7b,19b] The distorted coordination environment around Dy^{III} with the D_{4d} local symmetry, which is derived from the bpy ligand, lifts the 16-fold degeneracy of the J = 15/2 ground multiplet of Dy^{III}.[4e,24] The lowest doubly degenerate sublevels that formally correspond to large $J_z = \pm 15/2$[21] or $J_z = \pm 13/2$[4e,24] for dysprosium in the SAP environment are considerably separated from the rest of substates,[25] which can lead to a strong uniaxial magnetic anisotropy and a higher thermal barrier.[1c,d]

Compared with our previously reported similar complex of $[Dy(hfac)_3NIT\text{-}2Py]\cdot 0.5C_7H_{16}$ (NIT-2Py = 2-(2′-pyridyl)-4,4,5,5-tetramethylimidazoline-1-oxyl-3-oxide),[10c] which can show only slow magnetic relaxation behavior under a 1000 Oe external static magnetic field to suppress the quantum tunneling process, our Dy^{III} complex displays clear frequency dependence and peaks in χ' versus T and χ'' versus T plots in zero static field. In addition, our Dy^{III} complex has a significantly higher barrier of U = 38.48 K.

Static Magnetic Properties for ***2*** *and* ***3****.* The temperature dependence of magnetic susceptibilities for **2** and **3** is also studied and shown in Figure 7, and the $\chi_M T$ values at room temperature are 11.90 and 14.06 cm^3 K mol^{-1}, respectively. Both of the values are close to the expected values of 11.81 and 14.05 cm^3 K mol^{-1}, respectively, for one Ln^{III} ion ($^7F_6$, g = 3/2 for Tb^{III} and $^5I_8$, g = 5/4 for Ho^{III}). During the cooling process, the $\chi_M T$ values of **2** and **3** decrease gradually and reach a minimum of 8.47 and 7.43 cm^3 K mol^{-1} at 2 K, respectively. A strictly theoretical treatment of magnetic properties for such a system cannot be carried out because of the large anisotropy of the Ln^{III} ions. However, to obtain a rough quantitative estimate of the magnetic interaction parameters between paramagnetic species, we analyzed the temperature-dependent magnetic susceptibilities by an approximate model for **2** and **3**. The Ln^{III} ion may be assumed to exhibit a splitting of the m_j energy levels ($\hat{H} = \Delta \hat{J}_z^2$) in an axial crystal field.[26] Thus χ_{Tb} and χ_{Ho} can be described as eqs 1 and 2, respectively. In the expression, Δ is the zero-field-splitting parameter, g the Lande factor, k the Boltzmann constant, β the Bohr magneton constant, and N Avogadro's number. The zJ' parameter based on the molecular field approximation in eq 3 is introduced to simulate the magnetic interactions between all the paramagnetic species in the system.[27] Thus the magnetic data of **2** and **3** can be analyzed by the following approximate treatment of eqs 1−3.

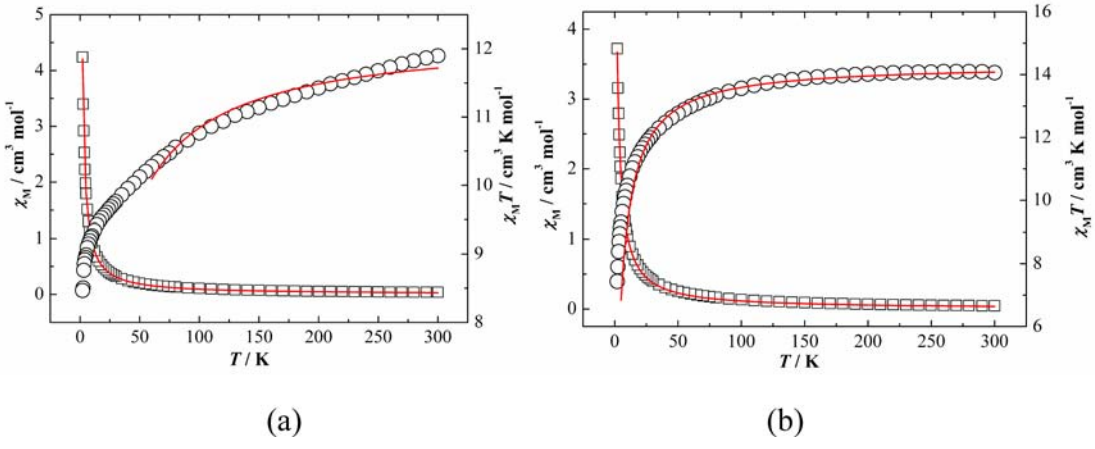

Figure 7. Temperature dependence of χ_M (□) and $\chi_M T$ (○) for Tb (**2**) (left) and Ho (**3**) (right) at 1000 Oe. The solid lines represent the theoretical values based on the corresponding equations.

dx.doi.org/10.1021/ic400006n | Inorg. Chem. 2013, 52, 7380−7386

$$\chi_{Tb} = \frac{2Ng^2\beta^2}{kT}\left\{\left[36\exp\left(\frac{-36\Delta}{kT}\right) + 25\exp\left(\frac{-25\Delta}{kT}\right) + 16\exp\left(\frac{-16\Delta}{kT}\right) + 9\exp\left(\frac{-9\Delta}{kT}\right) + 4\exp\left(\frac{-4\Delta}{kT}\right) + \exp\left(\frac{-\Delta}{kT}\right)\right]\Big/\left[2\exp\left(\frac{-36\Delta}{kT}\right) + 2\exp\left(\frac{-25\Delta}{kT}\right) + 2\exp\left(\frac{-16\Delta}{kT}\right) + 2\exp\left(\frac{-9\Delta}{kT}\right) + 2\exp\left(\frac{-4\Delta}{kT}\right) + 2\exp\left(\frac{-\Delta}{kT}\right) + 1\right]\right\} \quad (1)$$

$$\chi_{Ho} = \frac{2Ng^2\beta^2}{kT}\left\{\left[64\exp\left(\frac{-64\Delta}{kT}\right) + 49\exp\left(\frac{-49\Delta}{kT}\right) + 36\exp\left(\frac{-36\Delta}{kT}\right) + 25\exp\left(\frac{-25\Delta}{kT}\right) + 16\exp\left(\frac{-16\Delta}{kT}\right) + 9\exp\left(\frac{-9\Delta}{kT}\right) + 4\exp\left(\frac{-4\Delta}{kT}\right) + \exp\left(\frac{-\Delta}{kT}\right)\right]\Big/\left[2\exp\left(\frac{-64\Delta}{kT}\right) + 2\exp\left(\frac{-49\Delta}{kT}\right) + 2\exp\left(\frac{-36\Delta}{kT}\right) + 2\exp\left(\frac{-25\Delta}{kT}\right) + 2\exp\left(\frac{-16\Delta}{kT}\right) + 2\exp\left(\frac{-9\Delta}{kT}\right) + 2\exp\left(\frac{-4\Delta}{kT}\right) + 2\exp\left(\frac{-\Delta}{kT}\right) + 1\right]\right\} \quad (2)$$

$$\chi_M = \frac{\chi_{(Tb\text{ or }Ho)}}{1 - (2zJ'/Ng^2\beta^2)\chi_{(Tb\text{ or }Ho)}} \quad (3)$$

The best fitting parameters for Tb^{III} complex **2** are $g = 1.525$, $\Delta = 0.002\ cm^{-1}$, $zJ' = -0.312\ cm^{-1}$. For Ho^{III} complex **3**, they are $g = 1.262$, $\Delta = 0.009\ cm^{-1}$, $zJ' = -0.076\ cm^{-1}$. The very small zJ' values are indicative of the very weak magnetic interaction between Ln^{III} ions in **2** and **3**.

Tb^{III} and Ho^{III} complexes always have the tendency to be SMMs; therefore we performed the dynamic magnetic susceptibility measurements of the Tb^{III} complex **2** and the Ho^{III} complex **3**, which are given in the Supporting Information, Figures S6 and S7. Unfortunately, the imaginary component χ_M'' of the complexes does not show any positive value even at 2.0 K under zero-dc field. Thus, we do not think complexes **2** and **3** express SMM behavior even at low temperature. This may be due to the small energy barrier which could not prevent the inversion of the spin.[28]

CONCLUSIONS

In summary, we used 2,2′-bipyridine as the ancillary ligand of $Ln(hfac)_3{\cdot}2H_2O$ and successfully synthesized a single-ion magnet containing a Dy^{III} ion with approximate D_{4d} local symmetry. This Dy-based SIM has an energy barrier of 38.48 K to relax and a quantum regime of relaxation below 3 K, and both the Dy^{III} and Tb^{III} complexes have the typical luminescence peaks. We propose that the local symmetry of the center ions could modify the character of the magnetic relaxation. Further in-depth studies on the compounds of this kind are required to better understand the relaxation dynamics.

ASSOCIATED CONTENT

Supporting Information

X-ray crystallographic data for complexes **1**−**3** in CIF format, selected bond lengths and angles, figures of crystal structures, luminescence measurements, and magnetic measurements. This material is available free of charge via the Internet at http://pubs.acs.org.

AUTHOR INFORMATION

Corresponding Author

* E-mail: maynk@nankai.edu.cn (Y.M.), tang@ciac.jl.cn (J.T.).

Notes

The authors declare no competing financial interest.

ACKNOWLEDGMENTS

This work was supported by the National Natural Science Foundation of China (21101096, 90922032, 91022009, 21071085, and 91122013) and the Research Fund for the Doctoral Program of Higher Education (20100031120013 and 20120031130001).

REFERENCES

(1) (a) Carlin, R. L. *Magnetochemistry*; Springer: Berlin, 1986. (b) Gatteschi, D.; Sessoli, R.; Villain, J. *Molecular Nanomagnets*; Oxford University Press: New York, 2006. (c) Sorace, L.; Benelli, C.; Gatteschi, D. *Chem. Soc. Rev.* **2011**, *40*, 3092−3104. (d) Sessoli, R.; Powell, A. K. *Coord. Chem. Rev.* **2009**, *253*, 2328−2341. (e) Bi, Y.; Guo, Y. N.; Zhao, L.; Guo, Y.; Lin, S. Y.; Jiang, S. D.; Tang, J. K.; Wang, B. W.; Gao, S. *Chem.—Eur. J.* **2011**, *17*, 12476−12481. (f) Takamatsu, S.; Ishikawa, T.; Koshihara, S. Y.; Ishikawa, N. *Inorg. Chem.* **2007**, *46*, 7250−7252.

(2) (a) Ishikawa, N.; Sugita, M.; Ishikawa, T.; Koshihara, S.; Kaizu, Y. *J. Am. Chem. Soc.* **2003**, *125*, 8694−8695. (b) Ishikawa, N.; Sugita, M.; Ishikawa, T.; Koshihara, S.; Kaizu, Y. *J. Phys. Chem. B* **2004**, *108*, 11265−11271. (c) Ishikawa, N.; Mizuno, Y.; Takamatsu, S.; Ishikawa, T.; Koshihara, S. Y. *Inorg. Chem.* **2008**, *47*, 10217−10219.

(3) (a) Aldamen, M. A.; Clemente-Juan, J. M.; Coronado, E.; Martí-Gastaldo, C.; Gita-Ariño, A. *J. Am. Chem. Soc.* **2008**, *130*, 8874−8875. (b) AlDamen, M. A.; Cardona-Serra, S.; Clemente-Juan, J. M.; Coronado, E.; Gaita-Arino, A.; Marti-Gastaldo, C.; Luis, F.; Montero, O. *Inorg. Chem.* **2009**, *48*, 3467−3479.

(4) (a) Rinehart, J. D.; Long, J. R. *J. Am. Chem. Soc.* **2009**, *131*, 12558−12559. (b) Rinehart, J. D.; Meihaus, K. R.; Long, J. R. *J. Am. Chem. Soc.* **2010**, *132*, 7572−7573. (c) Ruiz, J.; Mota, A. J.; Rodriguez-Dieguez, A.; Titos, S.; Herrera, J. M.; Ruiz, E.; Cremades, E.; Costes, J. P.; Colacio, E. *Chem. Commun. (Cambridge, U.K.)* **2012**, *48*, 7916−7918. (d) Cucinotta, G.; Perfetti, M.; Luzon, J.; Etienne, M.; Car, P.; Caneschi, A.; Calvez, G.; Bernot, K.; Sessoli, R. *Angew. Chem., Int. Ed.* **2012**, *51*, 1606−1610. (e) Rinehart, J. D.; Long, J. R. *Chem. Sci.* **2011**, *2*, 2078−2085.

(5) (a) Cardona-Serra, S.; Clemente-Juan, J. M.; Coronado, E.; Gaita-Arino, A.; Camon, A.; Evangelisti, M.; Luis, F.; Martinez-Perez, M. J.; Sese, J. *J. Am. Chem. Soc.* **2012**, *134*, 14982−14990. (b) Luis, F.; Martínez-Pérez, M.; Montero, O.; Coronado, E.; Cardona-Serra, S.; Martí-Gastaldo, C.; Clemente-Juan, J. M.; Sesé, J.; Drung, D.; Schurig, T. *Phys. Rev. B* **2010**, *82*, 060403.

(6) (a) Yamashita, A.; Watanabe, A.; Akine, S.; Nabeshima, T.; Nakano, M.; Yamamura, T.; Kajiwara, T. *Angew. Chem., Int. Ed.* **2011**, *50*, 4016−4019. (b) Feltham, H. L. C.; Lan, Y. H.; Klçwer, F.; Ungur, L.; Chibotaru, L. F.; Powell, A. K.; Brooker, S. *Chem.—Eur. J.* **2011**, *17*, 4362−4365.

(7) (a) Chen, G. J.; Gao, C. Y.; Tian, J. L.; Tang, J. K.; Gu, W.; Liu, X.; Yan, S. P.; Liao, D. Z.; Cheng, P. *Dalton Trans.* **2011**, *40*, 5579−5583. (b) Jiang, S. D.; Wang, B. W.; Su, G.; Wang, Z. M.; Gao, S. *Angew. Chem., Int. Ed.* **2010**, *49*, 7448−7451. (c) Chen, G. J.; Guo, Y.

N.; Tian, J. L.; Tang, J. K.; Gu, W.; Liu, X.; Yan, S. P.; Cheng, P.; Liao, D. Z. *Chem.—Eur. J.* **2012**, *18*, 2484−2487.
(8) (a) Li, D. P.; Wang, T. W.; Li, C. H.; Liu, D. S.; Li, Y. Z.; You, X. Z. *Chem. Commun.* **2010**, *46*, 2929−2931. (b) Wang, Y.; Li, X. L.; Wang, T. W.; Song, Y.; You, X. Z. *Inorg. Chem.* **2010**, *49*, 969−976. (c) Liu, J.; Zhang, X. P.; Wu, T.; Ma, B. B.; Wang, T. W.; Li, C. H.; Li, Y. Z.; You, X. Z. *Inorg. Chem.* **2012**, *51*, 8649−8651.
(9) (a) Jiang, S. D.; Wang, B. W.; Sun, H. L.; Wang, Z. M.; Gao, S. *J. Am. Chem. Soc.* **2011**, *133*, 4730−4733. (b) Jiang, S. D.; Liu, S. S.; Zhou, L. N.; Wang, B. W.; Wang, Z. M.; Gao, S. *Inorg. Chem.* **2012**, *51*, 3079−3087.
(10) (a) Bernot, K.; Luzon, J.; Bogani, L.; Etienne, M.; Sangregorio, C.; Shanmugam, M.; Caneschi, A.; Sessoli, R.; Gatteschi, D. *J. Am. Chem. Soc.* **2009**, *131*, 5573−5579. (b) Bernot, K.; Pointillart, F.; Rosa, P.; Etienne, M.; Sessoli, R.; Gatteschi, D. *Chem. Commun.* **2010**, *46*, 6458−6460. (c) Wang, X. L.; Li, L. C.; Liao, D. Z. *Inorg. Chem.* **2010**, *49*, 4735−4737. (d) Zhou, N.; Ma, Y.; Wang, C.; Xu, G. F.; Tang, J. K.; Xu, J. X.; Yan, S. P.; Cheng, P.; Li, L. C.; Liao, D. Z. *Dalton Trans.* **2009**, 8489−8492. (e) Mei, X. L.; Ma, Y.; Li, L. C.; Liao, D. Z. *Dalton Trans.* **2012**, *41*, 505−511.
(11) Mori, F.; Nyui, T.; Ishida, T.; Nogami, T.; Choi, K. Y.; Nojiri, H. *J. Am. Chem. Soc.* **2006**, *128*, 1440−1441.
(12) (a) Armelao, L.; Quici, S.; Barigelletti, F.; Accorsi, G.; Bottaro, G.; Cavazzini, M.; Tondello, E. *Coord. Chem. Rev.* **2010**, *254*, 487−505. (b) Burrow, C. E.; Burchell, T. J.; Lin, P. H.; Habib, F.; Wernsdorfer, W.; Clerac, R.; Murugesu, M. *Inorg. Chem.* **2009**, *48*, 8051−8053. (c) Swavey, S.; Swavey, R. *Coord. Chem. Rev.* **2009**, *253*, 2627−2638. (d) van Staveren, D. R.; van Albada, G. A.; Haasnoot, J. G.; Kooijman, H.; Lanfredi, A. M. M.; Nieuwenhuizen, P. J.; Spek, A. L.; Ugozzoli, F.; Weyhermuller, T.; Reedijk, J. *Inorg. Chim. Acta* **2001**, *315*, 163−171. (e) Ahmed, Z.; Iftikhar, K. *Inorg. Chim. Acta* **2012**, *392*, 165−176. (f) Tang, S. F.; Mudring, A. V. *Eur. J. Inorg. Chem.* **2009**, 2769−2775. (g) Eliseeva, S. V.; Pleshkov, D. N.; Lyssenko, K. A.; Lepnev, L. S.; Bunzli, J. C. G.; Kuzmina, N. P. *Inorg. Chem.* **2011**, *50*, 5137−5144. (h) Zaim, A.; Favera, N. D.; Guenee, L.; Nozary, H.; Hoang, T. N. Y.; Eliseeva, S. V.; Petoud, S.; Piguet, C. *Chem. Sci.* **2013**, *4*, 1125−1136. (i) Eliseeva, S. V.; Kotova, O. V.; Gumy, F.; Semenov, S. N.; Kessler, V. G.; Lepnev, L. S.; Bunzli, J. C. G.; Kuzmina, N. P. *J. Phys. Chem. A* **2008**, *112*, 3614−3626. (j) Eliseeva, S. V.; Pleshkov, D. N.; Lyssenko, K. A.; Lepnev, L. S.; Bunzli, J. C. G.; Kuzmina, N. P. *Inorg. Chem.* **2010**, *49*, 9300−9311. (k) Eliseeva, S. V.; Bunzli, J. C. G. *Chem. Soc. Rev.* **2010**, *39*, 189−227. (l) Melby, L. R.; Rose, N. J.; Abramson, E.; Caris, J. C. *J. Am. Chem. Soc.* **1964**, *86*, 5117−5125.
(13) (a) *Theory and Applications of Molecular Paramagnetism*; Boudreaux, E. A., Mulay, L. N., Eds.; Wiley-Interscience: New York, 1976. (b) Bain, G. A.; Berry, J. F. *J. Chem. Educ.* **2008**, *85*, 532−536.
(14) (a) Sheldrick, G. M. *SHELXS-97, Program for the Solution of Crystal Structures*; University of Göttingen: Göttingen, Germany, 1997. (b) Sheldrick, G. M. *SHELXL-97, Program for the Refinement of Crystal Structures*; University of Göttingen: Göttingen, Germany, 1997.
(15) (a) Shiga, T.; Ohba, M.; Okawa, H. *Inorg. Chem. Commun.* **2003**, *6*, 15−18. (b) Akine, S.; Matsumoto, T.; Taniguchi, T.; Nabeshima, T. *Inorg. Chem.* **2005**, *44*, 3270−3274.
(16) (a) Muetterties, E. L.; Guggenberger, L. J. *J. Am. Chem. Soc.* **1974**, *96*, 1748−1756. (b) Tsukuda, T.; Suzuki, T.; Kaizaki, S. *Inorg. Chim. Acta* **2005**, *358*, 1253−1257.
(17) Hewitt, I. J.; Tang, J. K.; Madhu, N. T.; Anson, C. E.; Lan, Y. H.; Luzon, J.; Etienne, M.; Sessoli, R.; Powell, A. K. *Angew. Chem., Int. Ed.* **2010**, *49*, 6352−6356.
(18) (a) Osa, S.; Kido, T.; Matsumoto, N.; Re, N.; Pochaba, A.; Mrozinski, J. *J. Am. Chem. Soc.* **2004**, *126*, 420−421. (b) Guo, Y. N.; Chen, X. H.; Xue, S. F.; Tang, J. K. *Inorg. Chem.* **2011**, *50*, 9705−9713.
(19) (a) Ishikawa, N.; Sugita, M.; Wernsdorfer, W. *Angew. Chem., Int. Ed.* **2005**, *44*, 2931−2935. (b) Giraud, R.; Wernsdorfer, W.; Tkachuk, A. M.; Mailly, D.; Barbara, B. *Phys. Rev. Lett.* **2001**, *87*, 057203.
(20) Lin, P. H.; Burchell, T. J.; Ungur, L.; Chibotaru, L. F.; Wernsdorfer, W.; Murugesu, M. *Angew. Chem., Int. Ed.* **2009**, *48*, 9489−9492.
(21) (a) Cole, K. S.; Cole, R. H. *J. Chem. Phys.* **1941**, *9*, 341−351. (b) Aubin, S. M. J.; Sun, Z.; Pardi, L.; Krzystek, J.; Folting, K.; Brunel, L. C.; Rheingold, A. L.; Christou, G.; Hendrickson, D. N. *Inorg. Chem.* **1999**, *38*, 5329−5340.
(22) (a) Mydosh, J. A. *Spin Glasses: An Experimental Introduction*; Taylor & Francis: London, 1993. (b) Buschmann, W. E.; Ensling, J.; Gütlich, P.; Miller, J. S. *Chem.—Eur. J.* **1999**, *5*, 3019−3028.
(23) Yamaguchi, T.; Sunatsuki, Y.; Ishida, H.; Kojima, M.; Akashi, H.; Re, N.; Matsumoto, N.; Pochaba, A.; Mroziński, J. *Inorg. Chem.* **2008**, *47*, 5736−5745.
(24) Ishikawa, N. *Polyhedron* **2007**, *26*, 2147−2153.
(25) Pointillart, F.; Bernot, K.; Sessoli, R.; Gatteschi, D. *Chem.—Eur. J.* **2007**, *13*, 1602−1609.
(26) (a) Kahwa, I. A.; Selbin, J.; O'Connor, C. J.; Foise, J. W.; McPherson, G. L. *Inorg. Chim. Acta* **1988**, *148*, 265−272. (b) Xu, J. X.; Ma, Y.; Liao, D. Z.; Xu, G. F.; Tang, J. K.; Wang, C.; Zhou, N.; Yan, S. P.; Cheng, P.; Li, L. C. *Inorg. Chem.* **2009**, *48*, 8890−8896. (c) Wang, Y. L.; Zhou, N.; Ma, Y.; Qin, Z. X.; Wang, Q. L.; Li, L. C.; Cheng, P.; Liao, D. Z. *CrystEngComm* **2012**, *14*, 235−239. (d) Ouyang, Y.; Zhang, W.; Xu, N.; Xu, G. F.; Liao, D. Z.; Yoshimura, K.; Yan, S. P.; Cheng, P. *Inorg. Chem.* **2007**, *46*, 8454−8456. (e) Xu, N.; Shi, W.; Liao, D. Z.; Yan, S. P.; Cheng, P. *Inorg. Chem.* **2008**, *47*, 8748−8756. (f) Wang, Y. L.; Gao, Y. Y.; Ma, Y.; Wang, Q. L.; Li, L. C.; Liao, D. Z. *CrystEngComm* **2012**, *14*, 4706−4712.
(27) Liao, Y.; Shum, W. W.; Miller, J. S. *J. Am. Chem. Soc.* **2002**, *124*, 9336−9337.
(28) (a) Kajiwara, T.; Takahashi, K.; Hiraizumi, T.; Takaishi, S.; Yamashita, M. *CrystEngComm* **2009**, *11*, 2110−2116. (b) Kajiwara, T.; Nakano, M.; Takahashi, K.; Takaishi, S.; Yamashita, M. *Chem.—Eur. J.* **2011**, *17*, 196−205.